

# Deep tissue imaging with multiphoton fluorescence microscopy

David R. Miller<sup>1</sup>, Jeremy W. Jarrett<sup>1</sup>, Ahmed M. Hassan<sup>1</sup> and Andrew K. Dunn

## Abstract

We present a review of imaging deep-tissue structures with multiphoton microscopy. We examine the effects of light scattering and absorption due to the optical properties of biological sample and identify 1300 nm and 1700 nm as ideal excitation wavelengths. We summarize the availability of fluorophores for multiphoton microscopy as well as ultrafast laser sources to excite available fluorophores. Lastly, we discuss the applications of multiphoton microscopy for neuroscience.

## Addresses

Department of Biomedical Engineering, The University of Texas at Austin, 107 W. Dean Keeton C0800, Austin, TX 78712, USA

Corresponding author: Dunn, Andrew K. ([adunn@utexas.edu](mailto:adunn@utexas.edu))

<sup>1</sup> These authors contributed equally to this manuscript.

Current Opinion in Biomedical Engineering 2017, 4:32–39

This review comes from a themed issue on **Neural Engineering**

Edited by **Christine Schmidt**

Received 5 July 2017, revised 8 September 2017, accepted 13 September 2017

<https://doi.org/10.1016/j.cobme.2017.09.004>

2468-4511/© 2017 Elsevier Inc. All rights reserved.

## Keywords

Multiphoton microscopy fluorescence imaging, Scattering and absorption in brain tissue, Laser sources for multiphoton microscopy, Fluorophores for multiphoton microscopy.

## Introduction

The quest for new techniques capable of rapid, three-dimensional imaging with cellular resolution in intact tissues has fueled rapid advances in optical microscopy. Two-photon fluorescence microscopy (2PM), developed in the 1990's [1], is the most widely adopted method for minimally invasive *in vivo* brain imaging due to its ability to image in three dimensions. Recent *in vivo* imaging of neuronal circuits [2–4] and vascular networks [5,6] in the brain with micron-scale resolution has revealed significant new insight into cortical function and organization. Three-dimensional multiphoton imaging is possible because of a nonlinear dependence on excitation intensity, which confines two-photon fluorescence generation to the focal volume [7]. The resulting imaging depth is significantly greater than in confocal

fluorescence microscopy due to the longer excitation wavelength [8] and the ability to detect multiply scattered emission photons. However, the imaging depth for most 2PM imaging studies is around 500  $\mu\text{m}$ , which is sufficient to image superficial cortical layers in rodent experiments. This limitation on penetration depth arises from light scattering and absorption of tissue, both of which are wavelength dependent.

Traditional 2PM relies on Ti:Sapphire (Ti:S) lasers because of their ability to output mode-locked ultrafast pulses with high average powers, and their ability to excite a variety of fluorophores with one-photon absorption peaks in the visible range. Due to their reliability and robustness, Ti:S lasers have served as the workhorse of 2PM for the last 25 years and are commercially available from multiple laser companies as turn-key systems. While 2PM with Ti:S lasers substantially increases imaging depth relative to other optical microscopy approaches like confocal microscopy, Ti:S lasers are not optimized for deep imaging. To push the imaging depth further and visualize the entire mouse cortex (which is about 1 mm thick) and beyond, many new tools have been developed.

To appreciate the recent development of tools that extend the imaging depth of 2PM, it is important to understand that the optical properties of the biological sample serve as the fundamental limiting factors for imaging depth. Both excitation light and emission light are attenuated by absorption and scattering in biological tissue. Scattering and absorption effects vary by wavelength; thus, approaches to extend imaging depth focus on optimizing the excitation wavelengths, emission wavelengths, or a combination of both. The development of longer wavelength laser sources aims to reduce the scattering of excitation light. The advent of brighter fluorophores aims to both increase the amount of excitation light absorbed by the fluorophore as well as increase the likelihood that the fluorophore emits a fluorescent photon after absorption, and red-shifted fluorophores reduce the scattering effects of the emission light.

## Role of tissue optical properties in imaging depth

Scattering and absorption, characterized by the scattering coefficient ( $\mu_s$ ) and the absorption coefficient

( $\mu_a$ ), respectively, impact imaging depth by attenuating both the excitation laser light and emitted fluorescence, ultimately reducing the number of signal photons that reach the detector. The amount of scattered light decreases with increasing wavelength; however, absorption due to water increases significantly near 1500 nm and beyond 1800 nm. Figure 1 illustrates this wavelength-dependent effect by showing the normalized fraction of photons (blue line) that reach a depth of 1 mm for wavelengths from 700 to 2400 nm. Any scattered excitation light does not contribute to the multiphoton absorption process, so the fraction of photons of wavelength,  $\lambda$ , reaching a depth,  $z$ , can be modeled as  $\exp[-(\mu_a(\lambda) + \mu_s(\lambda))z]$ . The wavelength dependence of absorption is governed by water absorption, while the wavelength dependence of scattering is significantly more complex and difficult to measure, but is commonly approximated as  $\mu_s(\lambda) = a/(1 - g)(\lambda/500)^{-b}$ , where  $g$  is the scattering anisotropy and is usually assumed to be approximately 0.9 for biological tissues [9]. Under this approximation, the scattering coefficient is determined by the values of  $a$  and  $b$ , which can vary considerably, even for brain tissue [9]. The scaling factor  $a$  and scattering power  $b$  are parameters used to characterize the scattering coefficient.

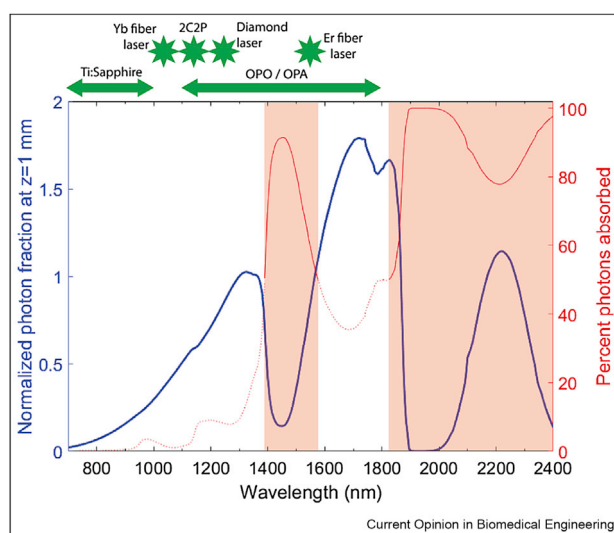
Figure 1 illustrates the contributions of scattering and absorption in biological tissue. The solid blue line is

calculated using average values for brain optical properties ( $g = 0.9$ ,  $a = 1.1 \text{ mm}^{-1}$ ,  $b = 1.37$ , water content = 75%) [9]. The plot demonstrates that 15 times more photons reach a depth of 1 mm using a wavelength of 1300 nm versus 800 nm, and 1.8 times more photons at 1700 nm versus 1300 nm. There is an additional peak near 2200 nm; however, it is in a red-shaded region indicating that more than 50% of the photons are absorbed by tissue. Although scattering and absorption attenuate photons with equal magnitude from a physics perspective, they are not equal from a physiological perspective. Excessive absorption is harmful to biological samples because it causes tissue heating. Wavelength regions in which >50% of photons are absorbed may not be viable for deep imaging without significant cause for concern due to excessive heating of tissue; thus, the peak at 2200 nm is not feasible for deep imaging. However, the peaks near 1300 nm and 1700 nm are viable and are the optimal wavelengths for deep imaging. At 1300 nm, conventional fluorophores may undergo two- or three-photon excitation depending on the fluorophore absorption characteristics, whereas most fluorophores undergo three-photon excitation at 1700 nm. We will use the term multiphoton microscopy (MPM) to collectively refer to fluorescence microscopy using two- or three-photon excitation, or any higher order excitation.

## Laser sources for deep imaging

Ti:S lasers have dominated the 2PM field because they reliably produce wavelength-tunable ultrafast pulses with high average power. Modern Ti:S lasers are robust, turn-key systems that enable routine 2PM imaging; however, they are not the optimal source for deep imaging within biological tissue. There are several approaches to increase imaging depth by reducing the effects of scattering in brain tissue while avoiding deleterious water absorption regions. A recent approach, adopted from astronomy, is the use of adaptive optics to shape the wavefront of excitation light to overcome tissue scattering [10]. An imaging depth of 700  $\mu\text{m}$  was reached in mouse cortex using adaptive optics [11]. Another approach is to increase the pulse energy of a laser source such that a greater number of photons per pulse penetrate to deeper tissue. Ti:S lasers typically produce pulse energies on the order of 10 nJ for repetition rates around 80 MHz. Using a Ti:S laser as a seed for a regenerative amplifier, pulse energies on the order of microjoules can be attained for repetition rates between 100 and 500 kHz. Using a regeneratively amplified Ti:S laser at a wavelength of 925 nm and repetition rate of 200 kHz, Theer *et al.* (2003) achieved an imaging depth of 1 mm [12]. A third approach to deep *in vivo* imaging is to use longer excitation wavelengths for which scattering effects are not as significant. Ti:S lasers typically have a wavelength maximum near 1000 nm. An optical parametric

Figure 1



**Effects of scattering and absorption.** Photon fraction at a depth of 1 mm for average brain tissue optical properties ( $g = 0.9$ ,  $a = 1.1 \text{ mm}^{-1}$ ,  $b = 1.37$ , water content = 75%) [9] is demarcated by the blue line. Regions shaded in red indicate areas in which 50% or more of photons are absorbed, as calculated by the red line (dashed red indicates below 50%; solid red indicates over 50%). Available laser options are outlined for their respective wavelength range (Yb = ytterbium, 2C2P = two-photon two-color of Yb fiber laser and diamond laser, Er = erbium, OPO = optical parametric oscillator, OPA = optical parametric amplifier).

oscillator (OPO), typically pumped by a Ti:S laser, offers a tunable wavelength range from  $\sim 1000$  nm to 1600 nm and beyond in some setups. Kobat *et al.* (2011) demonstrated an imaging depth of 1.6 mm using an OPO at 1280 nm with a pulse energy of 1.5 nJ [13]. A fourth approach is to utilize a long wavelength source with high pulse energy. An optical parametric amplifier (OPA) offers both a tunable wavelength range from  $\sim 1000$  nm to 1600 nm and pulse energies on the order of hundreds of nanojoules. Miller *et al.* (2017) demonstrated an imaging depth of 1.5 mm with an OPA at 1215 nm with a pulse energy of 400 nJ [14]. To achieve wavelengths near 1700 nm with high pulse energy, Horton *et al.* (2013) pumped a photonic-crystal rod with a 1550 nm erbium fiber laser to soliton self-frequency shift the wavelength to 1675 nm [8]. The output soliton had a pulse energy of 67 nJ, with which Horton *et al.* demonstrated an imaging depth of 1.4 mm.

Driven by advances in fiber laser technology, there are many turn-key systems that provide longer excitation wavelengths. Common systems include ytterbium fiber lasers ( $\lambda = 1030\text{--}1070$  nm, pulse energy = 1 nJ–40  $\mu$ J, repetition rate = 500 kHz–100 MHz) as well as fiber-laser-pumped optical parametric oscillators ( $\lambda = 1000\text{--}1600$  nm, pulse energy = 1 nJ–1 mJ, repetition rate = 1 kHz–80 MHz) and optical parametric amplifiers ( $\lambda = 1000\text{--}1600$  nm, pulse energy = 10 nJ–10  $\mu$ J, repetition rate = 1 kHz–10 MHz). These systems are being widely adopted for neuroscience investigations due to their reliability and increased imaging depth capabilities.

### Availability of fluorophores

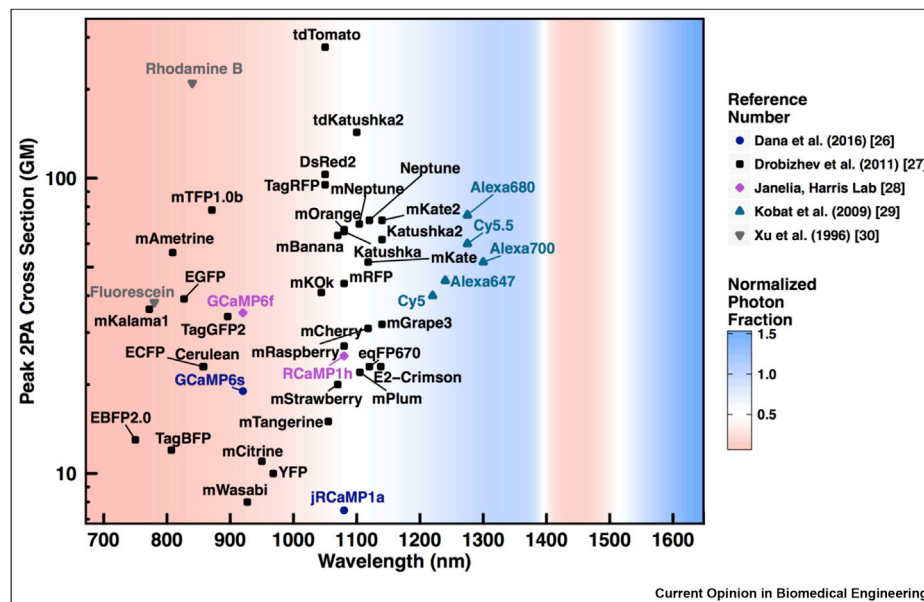
The discovery and development of bright, biocompatible contrast agents that excite at longer wavelengths is a crucial aspect to the advancement of *in vivo* MPM [15]. Fluorophores that excite near 1300 nm or 1700 nm are of particular interest due to minimal absorbance by water and reduced scattering. Exogenous fluorophores used for MPM can be categorized in two groups: organic and inorganic contrast agents [16]. The former class encompasses conventional organic dyes such as Texas red, fluorescein, and indocyanine green, which are extremely popular due to minimal aggregation issues and low cytotoxicity [17]. However, it is difficult to control the excitation and emission wavelengths of these dyes since their spectra are dependent on their chemical structure. In addition, fluorescent dyes commonly exhibit low quantum yields in aqueous environments, which reduces brightness in biological settings [16]. The latter category, inorganic probes, includes the well-established quantum dot, bright fluorescent semiconductor nanocrystals with broad absorption and discrete, tunable emission wavelengths that are highly resistant to photobleaching [18,19]. Recently, the polymer dot has emerged as an even

brighter, comparable alternative to quantum dots with decreased cytotoxicity [20–22]. Endogenous fluorescent proteins (FPs) offer a viable alternative to both organic and inorganic external contrast agents and can be used to label specific structures either by functionalization or genetic encoding. The selection of an appropriate FP for an imaging experiment involves careful consideration of factors such as brightness, photostability, and specificity [23]. In the past, the adoption of far-red variants of FPs has been obfuscated by their low brightness, but mKate, the pseudomonomeric tdKatushka2, and tdTomato collectively represent a new generation of bright, far-red emitters with substantial potential for deep *in vivo* imaging [24,25]. Figure 2 summarizes the peak two-photon absorption cross sections of various fluorophores reported in the literature.

Importantly, a probe can provide functionality beyond simply providing contrast; for instance, more sophisticated fluorescent sensors can be used to report on oxygen distributions *in vivo* [31,32] or monitor the activity of distinct neurons in brain tissue [33]. Indicators of neuronal activity rely on sensitivity to calcium ions (a proxy for action potentials), membrane potentials, or neurotransmitters [34]. In particular, genetically encoded calcium indicators (GECIs) have garnered attention and popularity within the neuroscience community despite challenges related to rapid calcium dynamics and low peak calcium accumulations [35]. Advances in protein engineering, structure based-design, and mutagenesis has produced a family of ultrasensitive protein calcium sensors (GCaMP6) that vastly outperform other indicators in terms of both sensitivity and reliability [36–38]. These sensors can be used to visualize large groups of neurons in addition to smaller synaptic protrusions, and remain stable for months [39]. The GCaMP6 family will undoubtedly be used to answer significant questions in neuroscientific research and recent work has even enabled functional imaging of the hippocampus at a  $\sim 1$  mm depth in mice [40]. Nevertheless, optimization of red GECIs has not kept pace with GFP-based designs and future research efforts will hopefully continue to improve the properties and application of these sensors [41].

Regardless of their function, characterization of the nonlinear properties of existing contrast agents to determine their compatibility with longer-wavelength excitation sources is a crucial first step towards their adoption as probes for MPM. There is a myriad of properties by which one can evaluate fluorophores, but action cross-section measurements, a product of absorption cross-section and quantum yield, are a particularly useful metric to evaluate brightness [42]. Unfortunately, accurate determination of cross-sections is a complicated endeavor that requires detailed information of the spectral properties of a chromophore,

Figure 2



**Cross sections of various fluorophores.** Peak two-photon absorption cross sections of common fluorophores compiled from published literature. Dark blue circles are from Dana *et al.* (2016) [26], black squares are from Drobizhev *et al.* (2011) [27], pink diamonds from Harris [28], teal triangles are from Kobat *et al.* (2009) [29], and gray inverted triangles are from Xu *et al.* (1996) [30]. The calculated normalized photon fraction of excitation light that reaches 1 mm into brain tissue (normalized to 1300 nm, analogous to Figure 1 solid blue line) is overlaid as background fill, where the color scale ranges from 0.01 (red) to 0.5 (white) to 1.6 (blue).

sample concentration, and a well-characterized standard [27,43]. As a result, the nonlinear properties of very few fluorophores have been reported, and in those limited instances, analysis has been limited to nonphysiological solvents at wavelengths below 1300 nm [44–48]. This wavelength limitation is in part due to the absence of reliable longer wavelength, ultrafast laser systems; however, given recent technological advances, two- and three-photon cross section measurements near 1700 nm are now achievable. Thus, the MPM community is engaged in a broad push to report cross section values at higher order regimes in order to take full advantage of the potential of available contrast agents and optimize experimental designs. Such recent work has demonstrated three-photon imaging of Texas Red and RFP at 1700 nm [8], three-photon cross section measurements of fluorescein ( $\lambda = 1300$  nm), wtGFP ( $\lambda = 1300$  nm), indocyanine green ( $\lambda = 1550$  nm), and SR101 ( $\lambda = 1680$  nm), and four-photon cross section measurements of fluorescein ( $\lambda = 1680$  nm) and wtGFP ( $\lambda = 1680$  nm) [49,50]. Simultaneous efforts have focused on the development of compounds with enhanced multiphoton properties [51]. In addition, improved red-shifted calcium indicators with advantages for deep *in vivo* imaging are being designed to rival the sensitivity of GCaMP6 [26]. Together, the characterization of existing contrast agents and the development of novel chromophores for

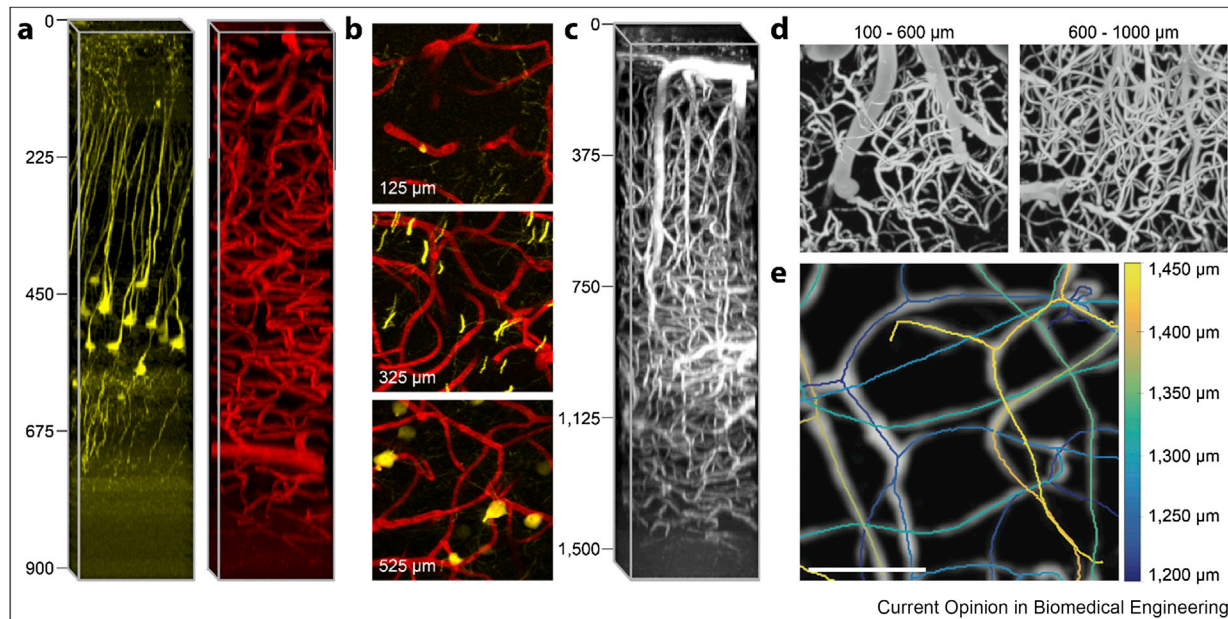
MPM will identify and produce probes that are sufficiently bright and photostable to overcome background fluorescence and scattering *in vivo*.

## Applications of deep multiphoton microscopy

MPM has been widely adopted by the neuroscience community due to its ability to perform minimally invasive three-dimensional imaging *in vivo* with cellular resolution. The imaging depth achievable with MPM has made it a powerful tool to study the morphology and dynamics of neuronal circuits and vascular networks in the rodent cortex. Due to the availability of longer wavelength excitation sources and brighter fluorophores with two-photon absorption peaks beyond 1000 nm, imaging depths beyond 500  $\mu$ m for MPM are becoming routine. Examples of deep tissue imaging obtained using recent technological advances described herein are presented in Figures 3 and 4. Figure 3 demonstrates deep imaging of vasculature and neuron morphology. In panels (a) and (b), an ytterbium fiber laser was used to simultaneously excite layer V pyramidal neurons transgenically labeled with YFP (B6.Cg-Tg(Thy1-YFP)HJrs/J) and vasculature perfused with Texas Red. In panels (c–e), an optical parametric amplifier was used to excite vasculature perfused with Texas Red; (e) demonstrates that vascular morphology can be vectorized for analysis at



Figure 3



**Examples of in vivo multiphoton microscopy.** (a) Image stacks of dimensions  $185 \times 185 \times 900 \mu\text{m}^3$  collected by two-photon excitation with an ytterbium-doped fiber laser labeling for layer V pyramidal neurons with YFP (left), and vasculature with Texas Red (right). (b) Merged z-projections of the stacks shown in a with neurons displayed in yellow and vasculature in red; the image at each plane is a maximum intensity projection of the nearest  $50 \mu\text{m}$ . (c) Image stack of dimensions  $365 \times 365 \times 1535 \text{ mm}^3$  collected by an optical parametric amplifier, labeling for vasculature with Texas Red. (d) Two-dimensional z-projections of the volume shown in c. (e) Vectorization of deep microvasculature in the volume shown in c. Scale bar is  $50 \mu\text{m}$ .

depths beyond 1 mm, enabling quantitative studies of vascular dynamics in deep-tissue structures. The examples presented in Figure 3 confirm the ability to visualize and track deep neurovascular structure.

Functionalized probes that reveal neural dynamics are enabling studies of neural circuits in the cortex and even the hippocampus. Recent work on this front by Ouzounov *et al.* (2017) is highlighted in Figure 4, which demonstrates functional imaging of CA1 hippocampal neurons labeled with GCaMP6s using an optical parametric amplifier at 1300 nm with a 55 fs pulse duration [40]. Panel (a) depicts the characteristic honeycomb arrangement of neurons found in the stratum pyramidale (SP) layer of a mouse hippocampus, and panel (b) shows fluorescence time traces from neurons labeled in (a), recorded at a frame rate of 8.49 Hz. Calcium transients due to spontaneous neural activity were clearly observed. CA1 hippocampal neurons have also been observed with a high-peak power gain-switched laser diode at 1064 nm with a 7.5 ps pulse duration [52]. Taken together, these results demonstrate the capability of current technology to acquire structural and functional neurovascular information with high spatial and temporal resolution deep within scattering brain tissue. The spatial resolution of MPM at depths

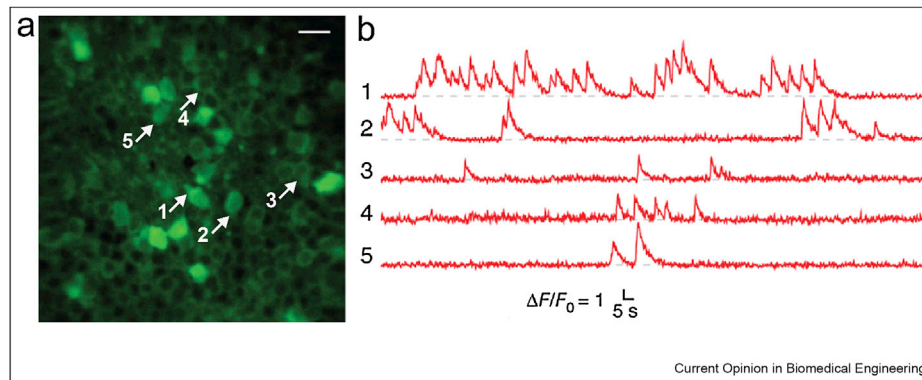
near 1 mm and beyond is an open question. There are a few reports of visualizations of dendrites beyond 1 mm [8,14,52], suggesting it may be possible to resolve dendritic spines and other fine features at depths greater than 1 mm. Adaptive optics may be a crucial aspect of this endeavor.

## Conclusion and future directions

To image deeper into highly scattering environments such as brain tissue, the MPM imaging community is trending toward using longer excitation wavelengths. We provide motivation for using excitation wavelengths near 1300 and 1700 nm. Future directions for MPM include the development of brighter fluorophores with peak brightness near these biological optical windows to enable reliable structural and functional imaging of the mouse cortex and deeper layers such as the hippocampus. Commercially available turn-key systems designed for deep imaging near 1300 and 1700 nm have recently become available and reliable, which will drive the adoption of MPM for neuroscience studies.

The extended penetration depth of multiphoton fluorescence imaging enabled by the synergistic development of longer wavelength systems and brighter, compatible fluorophores shapes a new paradigm in

Figure 4



**Recording of hippocampal neurons.** (a) Image of CA1 hippocampal neuron population from an 18–20 week old transgenic mouse (CAMKII-*tTA*/tetO-GCaMP6s) with a chronic cranial window preparation taken with three-photon microscopy at 984  $\mu\text{m}$  beneath the dura. Individual neurons are indexed for references to traces. Scale bar, 20  $\mu\text{m}$ . (b) Recording of spontaneous activity from labeled neurons in a. Reproduced with permission from Ouzounov *et al.* (2017) [40].

optical microscopy. No longer will optical microscopy be limited to the observation of cell monolayers, shallow tissue, or transparent biological organism. Rather, MPM may be used to examine previously inaccessible layers of tissue anatomy, such as the corpus callosum and hippocampus of mouse brain, and used to more readily probe optically dense samples including connective tissue, skin, lymph node, muscle, kidney, and tumors. In particular, tumor disease diagnosis will undoubtedly experience gains in sensitivity and specificity as imaging depth and signal-to-background ratio are improved. In the absence of efficient fluorophore excitation, investigators are forced to compensate by increasing laser power levels and risking photodamage to highly sensitive cell and tissue functions, including cell migration and signaling. Eliminating the need for dangerously high laser power levels will allow us to observe these processes unperturbed.

With these accomplishments in MPM, the next frontier for high resolution neuroimaging is the combination of optical imaging with photostimulation (i.e. calcium imaging channel rhodopsins). With future technology improvements in lasers and fluorophores, MPM will continue to play a vital role in neuroscience investigations of rodents and move into higher level vertebrates.

## Acknowledgements

The authors thank Dr. Evan Perillo, Taylor Clark, and Dr. Theresa Jones for assistance with imaging YFP mice, and Dr. Boris Zemelman for fruitful discussions on fluorescent proteins. This work is supported by the National Institutes of Health [NS082518, NS078791, EB011556]; the American Heart Association [14EIA18970041]; and the Cancer Prevention and Research Institute of Texas [RR160005]. David Miller is supported by the National Science Foundation Graduate Research Fellowship Program [DGE-1110007].

## Conflict of interest

None of the authors has any conflicts of interests.

## References

Papers of particular interest, published within the period of review, have been highlighted as:

- \* of special interest
- \*\* of outstanding interest

1. Denk W, Strickler JH, Webb WW: **Two-photon laser scanning fluorescence microscopy**. *Science* 1990, **248**:73–76.
2. Lin MZ, Schnitzer MJ: **Genetically encoded indicators of neuronal activity**. *Nat Neurosci* 2016, **19**:1142–1153.
3. Sofroniew NJ, Flickinger D, King J, Svoboda K: **A large field of view two-photon mesoscope with subcellular resolution for in vivo imaging**. *eLife* 2016, **5**, e14472.
4. Tischbirek C, Birkner A, Jia H, Sakamann B, Konnerth A: **Deep two-photon brain imaging with a red-shifted fluorometric  $\text{Ca}^{2+}$  indicator**. *Proc Natl Acad Sci USA* 2015, **112**: 11377–11382.
5. Tsai PS, Mateo C, Field JJ, Schaffer CB, Anderson ME, Kleinfeld D: **Ultra-large field-of-view two-photon microscopy**. *Opt Express* 2015, **23**:13833–13847.
6. Shih AY, Driscoll JD, Drew PJ, Nishimura N, Schaffer CB, Kleinfeld D: **Two-photon microscopy as a tool to study blood flow and neurovascular coupling in the rodent brain**. *J Cereb Blood Flow Metab* 2012, **32**:1277–1309.
7. Helmchen F, Denk W: **Deep tissue two-photon microscopy**. *Nat Methods* 2005, **2**:932–940.
8. Horton NG, Wang K, Kobat D, Clark CG, Wise FW, Schaffer CB, Xu C: **In vivo three-photon microscopy of subcortical structures within an intact mouse brain**. *Nat Photonics* 2013, **7**: 205–209.
9. Jacques SL: **Optical properties of biological tissues: a review**. *Phys Med Biol* 2013, **58**:R37–R61.
10. Kubby JA: **Adaptive optics for biological imaging**. CRC Press; 2013.
11. Wang K, Sun W, Richie CT, Harvey BK, Betzig E, Ji N: **Direct wavefront sensing for high-resolution in vivo imaging in scattering tissue**. *Nat Commun* 2015, **6**, 7276.

12. Theer P, Hasan MT, Denk W: **Two-photon imaging to a depth of 1000  $\mu\text{m}$  in living brains by use of  $\text{Ti:Al}_2\text{O}_3$  regenerative amplifier.** *Opt Lett* 2003, **28**:1022–1024.
13. Kobat D, Horton NG, Xu C: **In vivo two-photon microscopy to 1.6-mm depth in mouse cortex.** *J Biomed Opt* 2011, **16**: 106014-1–106014-4.
14. Miller DR, Hassan AM, Jarrett JW, Medina FA, Perillo EP, Hagan K, Kazmi SMS, Clark TA, Sullender CT, Jones TA, Zemelman BV, Dunn AK: **In vivo multiphoton imaging of a diverse array of fluorophores to investigate deep neurovascular structure.** *Biomed Opt Express* 2017, **8**: 3470–3481.
15. Kim HM, Cho BR: **Small-molecule two-photon probes for bioimaging applications.** *Chem Rev* 2015, **115**:5014–5055.  
\* This paper provides a comprehensive review of the design, synthesis, and biomedical application of probes for two-photon microscopy.
16. Frangioni JV: **In vivo near-infrared fluorescence imaging.** *Curr Opin Chem Biol* 2003, **7**:626–634.
17. Resch-Genger U, Grabolle M, Cavaliere-Jaricot S, Nitschke R, Nann T: **Quantum dots versus organic dyes as fluorescent labels.** *Nat Methods* 2008, **5**:763–775.
18. Larson DR, Zipfel WR, Williams RM, Clark SW, Bruchez MP, Wise FW, Webb WW: **Water-soluble quantum dots for multiphoton fluorescence imaging in vivo.** *Science* 2003, **300**: 1434–1436.
19. Medintz IL, Uyeda HT, Goldman ER, Mattoussi H: **Quantum dot bioconjugates for imaging, labelling and sensing.** *Nat Mater* 2005, **4**:435–446.
20. Changfeng W, Chiu DT: **Highly fluorescent semiconducting polymer dots for biology and medicine.** *Angew Chem Int Ed* 2013, **52**:3086–3109.
21. Changfeng W, Szymanski C, Cain Z, McNeill J: **Conjugated polymer dots for multiphoton fluorescence imaging.** *J Am Chem Soc* 2007, **129**:12904–12905.
22. Pecher J, Huber J, Winterhalder M, Zumbusch A, Mecking S: **Tailor-made conjugated polymer nanoparticles for multicolor and multiphoton cell imaging.** *Biomacromolecules* 2010, **11**: 2776–2780.
23. Shaner NC, Steinbach PA, Tsien RY: **A guide to choosing fluorescent proteins.** *Nat Methods* 2005, **2**:905–909.
24. Shcherbo D, Murphy CS, Ermakova GV, Solovieva EA, Chepurmykh TV, Shcheglov AS, Verkhusha VV, Pletnev VZ, Hazelwood KL, Roche PM, Lukyanov S: **Far-red fluorescent tags for protein imaging in living tissues.** *Biochem J* 2009, **15**: 567–574.
25. Bianchi R, Teixeira A, Proulx ST, Christiansen AJ, Seidel CD, Rüllicke T, Mäkinen T, Hägerling R, Halin C, Detmar M: **A transgenic Prox1-Cre-tdTomato reporter mouse for lymphatic vessel research.** *PLoS One* 2015, **10**, e0122976.
26. Dana H, Mohar B, Sun Y, Narayan S, Gordus A, Hasseman JP, Getahun T, Holt GT, Hu A, Walpita D, Patel R, et al.: **Sensitive red protein calcium indicators for imaging neural activity.** *eLife* 2016, **5**, e12727.  
\* This paper details the design and characterization of new, sensitive red genetically encoded calcium indicators that facilitate deep-tissue functional imaging.
27. Drobizhev M, Makarov NS, Tillo SE, Hughes TE, Rebane A: **Two-photon absorption properties of fluorescent proteins.** *Nat Methods* 2011, **8**:393–399.
28. Harris T. Two-photon fluorescent probes. URL: <https://www.janelia.org/lab/harris-lab/apig/research/photophysics/two-photon-fluorescent-probes>. [Accessed 12 June 2017].
29. Kobat D, Durst ME, Nishimura N, Wong AW, Schaffer CB, Xu C: **Deep tissue multiphoton microscopy using longer wavelength excitation.** *Opt Express* 2009, **17**:13354–13364.
30. Xu C, Webb WW: **Measurement of two-photon excitation cross sections of molecular fluorophores with data from 690 to 1050 nm.** *J Opt Soc Am B* 1996, **13**:481–491.
31. Finikova OS, Lebedev AY, Aprelev A, Troxler T, Gao F, Garnacho C, Muro S, Hochstrasser RM, Vinogradov SA: **Oxygen microscopy by two-photon-excited phosphorescence.** *ChemPhysChem* 2008, **9**:1673–1679.
32. Gagnon L, Sakadžić S, Lesage F, Musacchia JJ, Lefebvre J, Fang Q, Yücel MA, Evans KC, Mandeville ET, Cohen-Adad J, Polimeni JR, Yaseen MA, Lo EH, Greve DN, Buxton RB, Dale AM, Devor A, Boas DA: **Quantifying the microvascular origin of BOLD-fMRI from first principles with two-photon microscopy and an oxygen-sensitive nanoprobe.** *J Neurosci* 2015, **25**:3663–3675.  
\* Superb demonstration of large-volume experimental measurements of  $\text{pO}_2$  in vivo using 2PM of vasculature labeled with PtP-C343, the most well regarded oxygen-sensitive probe for 2PM.
33. Stosiek C, Garaschuk O, Holthoff K, Konnerth A: **In vivo two-photon calcium imaging of neuronal networks.** *Proc Natl Acad Sci USA* 2003, **100**:7319–7324.
34. Looger LL, Griesbeck O: **Genetically encoded neural activity indicators.** *Curr Opin Neurobiol* 2012, **22**:18–23.
35. Sabatini BL, Oertner TG, Svoboda K: **The life cycle of  $\text{Ca}^{2+}$  ions in dendritic spines.** *Neuron* 2002, **33**:439–452.
36. Tian L, Hires SA, Mao T, Huber D, Chiappe ME, Chalasani SH, Petreanu L, Akerboom J, McKinney SA, Schreiter ER, Bargmann CI: **Imaging neural activity in worms, flies and mice with improved GCaMP calcium indicators.** *Nat Methods* 2009, **6**:875–881.
37. Akerboom J, Chen TW, Wardill TJ, Tian L, Marvin JS, Mutlu S, Calderón NC, Esposti F, Borghuis BG, Sun XR, Gordus A: **Optimization of a GCaMP calcium indicator for neural activity imaging.** *J Neurosci* 2012, **32**:13819–13840.
38. Nakai J, Ohkura M, Imoto K: **A high signal-to-noise  $\text{Ca}^{2+}$  probe composed of a single green fluorescent protein.** *Nat Biotechnol* 2001, **19**:137–141.
39. Chen TW, Wardill TJ, Sun Y, Pulver SR, Renninger SL, Baohuan A, Schreiter ER, Kerr RA, Orger MB, Jayaraman V, Looger LL: **Ultrasensitive fluorescent proteins for imaging neuronal activity.** *Nature* 2013, **499**:25–300.
40. Ouzounov DG, Wang T, Wang M, Feng DD, Horton NG, Cruz-Hernández JC, Cheng YT, Reimer J, Tolias AS, Nishimura N, Xu C: **In vivo three-photon imaging of activity of GCaMP6-labeled neurons deep in intact mouse brain.** *Nat Methods* 2017, **14**:388–390.  
\* This paper demonstrates cutting-edge technical work and the enormous potential of three-photon imaging of optimized probes, which enable functional optical imaging of the hippocampus.
41. Inoue M, Takeuchi A, Horigane SI, Ohkura M, Gengyo-Ando K, Fujii H, Kamijo S, Takemoto-Kimura S, Kano M, Nakai J, Kitamura K, Bito H: **Rational design of a high-affinity, fast, red calcium indicator R-CaMP2.** *Nat Methods* 2015, **12**:64–70.
42. Xu C, Zipfel WR: **Multiphoton excitation of fluorescent probes.** *Cold Spring Harbor Protoc* 2015. <https://doi.org/10.1101/pdb.top086116>.  
\* This publication offers a rationale for the importance of evaluating the multiphoton action cross-sections of contrast agents and provides a thorough derivation through underlying physics. In addition, it contains a summary of multiphoton cross-section measurements of a variety of dyes, molecules, proteins, and quantum dots.
43. Mütze J, Iyer V, Macklin JJ, Colonell J, Karsh B, Petrášek Z, Schwillie P, Looger LL, Lavis LD, Harris TD: **Excitation spectra and brightness optimization of two-photon excited probes.** *Biophys J* 2012, **102**:934–944.
44. Kauert M, Stoller PC, Frenz M, Rieck J: **Absolute measurement of molecular two-photon absorption cross-sections using a fluorescence saturation technique.** *Opt Express* 2006, **14**: 8434–8447.
45. Oulianov DA, Tomov IV, Dvornikov AS, Rentzepis PM: **Observations on the measurement of two-photon absorption cross-section.** *Opt Commun* 2001, **191**:235–243.
46. Tian P, Warren WS: **Ultrafast measurement of two-photon absorption by loss modulation.** *Opt Lett* 2002, **27**:1634–1636.

47. Sengupta P, Balaji J, Banerjee S, Philip R, Kumar GR, Maiti S: **Sensitive measurement of absolute two-photon absorption cross sections.** *J Chem Phys* 2000, **112**:9201–9205.
48. Kapoor R, Friend CS, Patra A: **Two-photon-excited absolute emission cross-sectional measurements calibrated with a luminance meter.** *J Opt Soc Am B* 2003, **20**:1550–1554.
49. Cheng LC, Horton NG, Wang K, Chen SJ, Xu C: **Measurements of multiphoton action cross section for multiphoton microscopy.** *Biomed Opt Express* 2014, **5**:3427–3433.
50. Berezin MY, Zhan C, Lee H, Joo C, Akers WJ, Yazdanfar S, Achilefu S: **Two-photon optical properties of near-infrared dyes at 1.55  $\mu\text{m}$  excitation.** *J Phys Chem B* 2011, **115**:11530–11535.
51. Le Droumaguet C, Mongin O, Werts MHV, Blanchard-Desce M: **Towards “smart” multiphoton fluorophores: strongly solvatochromic probes for two-photon sensing of micropolarity.** *Chem Commun* 2005:2802–2804.
52. Kawakami R, Sawada K, Kusama Y, Fang Y, Kanazawa S, Kozawa Y, Sato S, Yokoyama H, Nemoto T: ***In vivo* two-photon imaging of mouse hippocampal neurons in dentate gyrus using a light source based on a high-peak power gain-switched laser diode.** *Biomed Opt Express* 2015, **6**:891–901.